Hydrogen adsorption on GaAs (001) reconstructions

R. F. Hicks,[a] H. Qi, Q. Fu, B.-K. Han, and L. Li
Chemical Engineering Department, University of California, Los Angeles, Los Angeles, California 90095-1592

(Received 14 January 1999; accepted 9 March 1999)

Hydrogen adsorption on the $c(4\times4)$, (2×4), (2×6), and (4×2) reconstructions of GaAs (001) have been characterized by internal-reflection infrared spectroscopy. The infrared spectra contain up to 15 bands due to the stretching vibrations of arsenic hydrides (2150–1950 cm^{-1}), terminal gallium hydrides (1950–1800 cm^{-1}), and bridging gallium hydrides (1800–950 cm^{-1}). These features arise from hydrogen adsorption on arsenic and gallium dimers, and second-layer arsenic and gallium atoms. The large number of peaks observed indicates that the surface atoms exist in a variety of different chemical environments. © *1999 American Institute of Physics.*
[S0021-9606(99)71321-8]

I. INTRODUCTION

Gallium arsenide (001) has been widely studied because it is used to manufacture many important semiconductor devices, and because it exhibits a variety of interesting surface structures.[1–12] The GaAs (001) surface can be terminated with either arsenic or gallium. In order to minimize the surface free energy, the As and Ga atoms form dimers, leaving only one dangling bond per atom. On charge-neutral surfaces, the arsenic dangling bonds are filled with pairs of electrons, while the gallium dangling bonds are empty.[13] This charge-neutral condition is achieved by removing some fraction of the As or Ga dimers from the top layer of each unit cell.

As the surface composition changes from an arsenic-rich to a gallium-rich state, the surface undergoes at least four different reconstructions.[3,5,10,12] Shown in Fig. 1 are ball-and-stick models that have been proposed for each reconstruction. Model (a) is the $c(4\times4)$ structure which occurs at an arsenic coverage of 1.75 monolayers (ML).[3] On this surface, three-quarters of a monolayer of As is adsorbed on top of the first layer of arsenic. The extra As atoms dimerize in the [110] direction. Hashizume *et al.*[5] have obtained scanning tunneling micrographs of the $c(4\times4)$ surface, which show dimer chains varying in length from 1 to 3 units [only 3 are shown in model (a)]. The shorter chains must occur when the As coverage is below 1.75 ML.

Pashley *et al.*[4] obtained the first scanning tunneling micrographs of the (2×4) reconstruction, which occurs at an As coverage of 0.75 ML. Their images are consistent with three arsenic dimers in the first layer followed by one dimer vacancy [model (b), Fig. 1]. On this surface, the As dimer bonds are parallel to the [110] direction. The out-of-phase alignment of adjacent (2×4) cells gives rise to a larger $c(2\times8)$ unit cell. Biegelsen *et al.*[3] observed another (2×4) phase with two As dimers in the first layer and one As dimer in the third layer [model (c)]. Theoretical calculations have shown that model (c) is more energetically favorable than model (b).[7] Based on reflection high-energy electron diffraction (RHEED) measurements, Farrell *et al.*[14] suggested another (2×4) structure with two As dimers in the top layer and two Ga dimers in the trenches [model (d)]. The As coverage for this reconstruction is 0.5 ML.

On gallium-rich surfaces, the two reconstructions that are seen by low-energy electron diffraction (LEED) and scanning tunneling microscopy (STM) are the $(2\times6)/(1\times6)$ and $(4\times2)/c(8\times2)$. Model (e) in Fig. 1 shows the structure of the (2×6) as proposed by Biegelsen *et al.*[3] It consists of two rows of As dimers, separated by two rows of Ga dimers. The As and Ga dimer bonds are oriented along the [110] and [$\bar{1}$10] crystal axis, respectively. This structure occurs at an arsenic coverage of 0.5 ML. The presence of Ga dimers on the (2×6) surface has been confirmed by infrared spectroscopy of adsorbed hydrogen, which reveals a broad, low-frequency band due to bridging gallium hydride.[9]

Three models for the $(4\times2)/c(8\times2)$ reconstruction are presented in Fig. 1. Model (f), proposed by Frankel *et al.*,[15] contains three gallium dimers and a dimer vacancy, and corresponds to a Ga coverage of 0.75 ML. Model (h), proposed by Skala *et al.*,[16] contains two gallium dimers and two arsenic dimers, and corresponds to a Ga coverage of 0.50 ML. On the other hand, careful studies of the (4×2) using the STM have provided clear evidence that model (g), with two Ga dimers in the first layer and one Ga dimer in the third layer, is the correct representation of the surface.[3,5] This conclusion is further supported by total energy calculations.[7]

The structures presented in Fig. 1 are based on numerous studies of the GaAs (001) surfaces, using techniques such as x-ray scattering,[17] x-ray photoemission spectroscopy (XPS),[18–20] RHEED,[1,14,21–26] LEED,[11,12,27,28] Auger electron spectroscopy (AES),[12,15,29] high-resolution electron energy loss spectroscopy (HREELS),[15,30,31] and STM.[3–6,10,16,32–34] Of these techniques, STM uniquely provides a map of the local density of states with atomic resolution. However, it is difficult to image the empty states on the GaAs (001) surface, i.e., the gallium sites. Since no Ga dimers have ever been clearly identified by STM, conflicting conclusions have been drawn from very similar images of the Ga-rich surfaces.[3–5,16]

We have used high-resolution vibrational spectroscopy

[a]Electronic mail: rhicks@ucla.edu

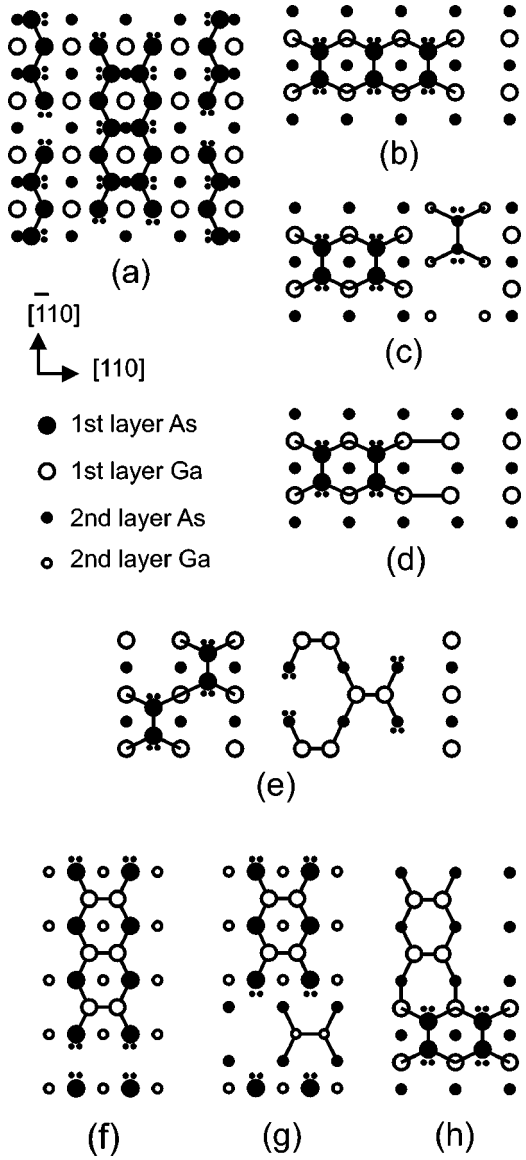

FIG. 1. Ball-and-stick models of GaAs (001) reconstructions reported in the literature. The lone pair of electrons in the As dangling bonds is indicated by two small dots.

to investigate the adsorption of hydrogen and other molecules on the (2×4) and (2×6) reconstructions of GaAs (001).[9,35] Hydrogen atoms bond to four main sites on these surfaces: As dimers, Ga dimers, second-layer As atoms, and second-layer Ga atoms. The second-layer atoms occupy lattice sites underneath the dimers, and are threefold coordinated with one remaining dangling bond. These sites are usually located along the edges of dimer vacancy rows. Each of the four sites is distinguished from each other by the frequencies of the hydride stretching vibrations in the infrared spectrum. An important discovery of this work was that hydrogen inserts into the Ga dimers, forming bridging gallium hydrides that are held via 3-center-2-electron bonds.[9]

In this paper, we have extended our earlier studies of hydrogen adsorption on GaAs (001) to include all four reconstructions, the $c(4\times4)$, (2×4), (2×6), and (4×2). Moreover, the surfaces have been prepared by growing high-quality GaAs films on top of single-crystal substrates by metalorganic vapor-phase epitaxy.[10] Previously, we generated GaAs surfaces by wet chemical etching and annealing in vacuum.[9] All the surfaces prepared in this study have been characterized by LEED, XPS, and STM. Then the infrared spectra of adsorbed hydrogen were collected and the results compared directly to the data obtained by the other techniques.

We have found that on the $c(4\times4)$, the hydrogen atoms displace the top layer of arsenic dimers, and adsorb onto the As atoms underneath. Hydrogen adsorption on the As-rich $c(4\times4)$ and (2×4) surfaces produces seven distinct As–H vibrational bands. These bands are attributed to arsenic monohydrides with different chemical bond strengths. On the Ga-rich (2×6) and (4×2) reconstructions, the infrared spectra contain intense, broad bands between 1750 and 850 cm^{-1}, which are due to bridging gallium hydrides. This feature provides direct evidence for the presence of gallium dimers on these reconstructions. This study demonstrates that vibrational spectroscopy of adsorbed hydrogen is a valuable tool for probing compound semiconductor surfaces, since it provides a unique picture of the chemical environment associated with the dangling bonds on each reconstruction.

II. EXPERIMENTAL METHODS

Gallium arsenide films, 0.5 μm thick, were grown on GaAs (001) substrates using tertiarybutylarsine (TBAs), triethylgallium (TEGa), and hydrogen carrier gas. The growth conditions were: 873 K, 20 Torr H_2 pressure, 6.5×10^{-4} Torr TEGa pressure, a V/III ratio of 50, and a space velocity over the crystal of 30 cm/s (at 298 K and 760 Torr).[10] After growth, the crystal was held at 873 K for 5 min, then cooled to room temperature. The flows of tertiarybutylarsine and hydrogen were maintained until the temperature reached 473 and 300 K, respectively. Immediately after stopping the H_2 flow, the reactor was pumped out to 5×10^{-7} Torr, and the sample was transferred to an ultrahigh vacuum (UHV) system through an interface chamber without air exposure. The base pressure of the UHV system was 2×10^{-10} Torr. Next, the GaAs (001) crystals were annealed at various temperatures for 15 min to get the desired reconstructions.

The gallium arsenide reconstructions generated in ultrahigh vacuum were identified by low-energy electron diffraction, using a Princeton Instruments reverse-view LEED. The surface composition of each phase was measured with a PHI 5000 x-ray photoelectron spectrometer, equipped with a hemispherical analyzer. These spectra were recorded at a takeoff angle of 75° with respect to the sample normal, using Al K_α x-rays, and a pass energy of 35.75 eV. The scanning tunneling micrographs were obtained with a Park Scientific Instruments auto probe VP STM. The images were taken of the filled states at a sample bias of −2.0 to −4.0 V, and a tunneling current of 0.1 to 0.5 nA.

Infrared spectra were obtained by multiple internal reflection through GaAs (001) crystals that were 10 mm wide by 40 mm long by 0.64 mm thick, and with 45 deg bevels at each end. A total of 31 reflections occurred off the front face of the crystals. Two substrate orientations were used: one

TABLE I. The dependence of the GaAs (001) LEED pattern and XPS As/Ga area ratio on the annealing temperature in ultrahigh vacuum.

LEED pattern	As $2p_{3/2}$/Ga $2p_{3/2}$ area ratio	Annealing temperature (K)	Temperature range (K)
$c(4\times4)$	2.1–1.8	523	573–623
$c(2\times8)$	1.4–1.25	673	673–773
(1×6)	1.1	793	773–813
$c(8\times2)$	1.1–1.25	853	823–873

with the long crystal axis parallel to the $[\bar{1}10]$ direction, and one with the long crystal axis parallel to the $[110]$ direction. Hydrogen was dosed into the chamber at 5×10^{-7} Torr, and dissociated with a tungsten filament located 4 cm from the sample face. The flux of H atoms relative to H_2 molecules was estimated to be 0.1%.[9] Dosing was continued for 30 min (900 L H_2) to allow the hydrogen atoms to saturate the exposed sites on the semiconductor surface. A series of infrared spectra was collected before and during this exposure, using a Diglab FTS-40A Fourier-transform infrared spectrometer. The spectra were recorded at 8 cm^{-1} resolution and coadding 1024 scans. The reflectance spectra presented here were obtained by taking the ratio of the spectra taken at saturation coverage to that taken before hydrogen dosing.

The LEED, XPS, STM, and IR results reported in this paper were all collected at a sample temperature of 300 K.

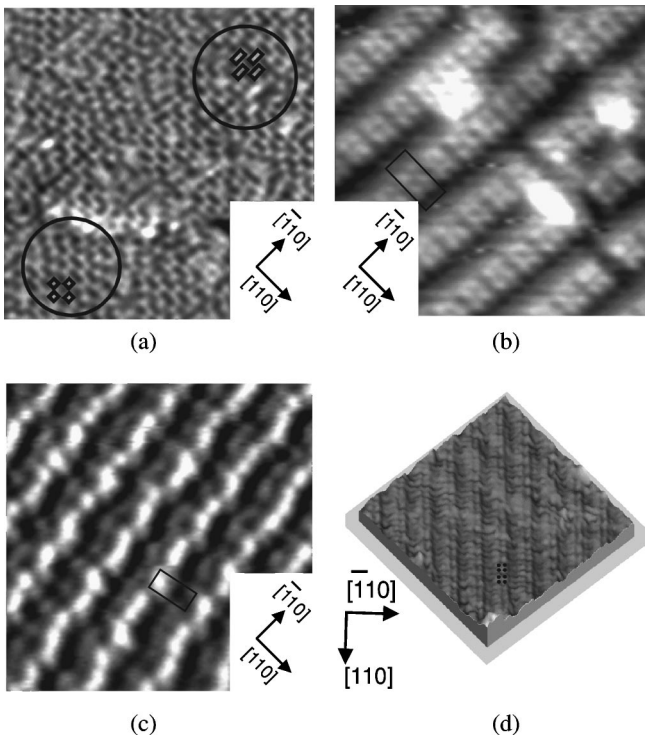

FIG. 2. Scanning tunneling micrographs of GaAs(001) reconstructions: (a) $c(4\times4)$, 200×200 Å^2; (b) (2×4), 80×80 Å^2; (c) (2×6), 140×140 Å^2; and (d) (4×2), 110×110 Å^2.

III. RESULTS

Immediately after removing a gallium arsenide sample from the metalorganic vapor phase epitaxy (MOVPE) reactor, its surface exhibits a disordered $c(4\times4)$ reconstruction, and contains a significant quantity of adsorbed hydrocarbons.[36] Slowly heating the sample to 623 K desorbs the hydrocarbons, and produces an ordered $c(4\times4)$ phase. Further heating to progressively higher temperatures results in arsenic desorption with the appearance of the $c(2\times8)$, (1×6), and last, $c(8\times2)$ LEED pattern. The annealing temperatures used to obtain these LEED patterns are listed in Table I. Also shown are the temperature ranges over which each reconstruction is observed, and the corresponding area ratios recorded for the As $2p_{3/2}$ and Ga $2p_{3/2}$ photoemission peaks. The temperature range for observing a particular structure depends on several factors, including the heating rate, the maximum temperature attained, and the annealing time. Therefore, these ranges are considered approximate and will not exactly match the annealing temperatures used in other studies. It should be noted that our heating rates were governed by the need to keep the chamber pressure below 1×10^{-9} Torr, and were between 3 and 5 K/min.

The XPS area ratios presented in Table I are not corrected for the atomic sensitivity factors, because these factors are analyzer dependent and we are using the ratios only as a relative measure of the surface composition. Inspection of the XPS data reveals that the As/Ga area ratio is a minimum for the $(1\times6)/(2\times6)$ reconstruction. This is consistent with the (2×6) and (4×2) structures as given by models (e) and (g) in Fig. 1. The mean free path for the escaping photoelectrons from the As and Ga $2p_{3/2}$ levels are 7 and 10 Å, respectively, which is between 5 and 7 atomic layers of the GaAs crystal.[37] The ratios of the number of As atoms to Ga atoms in the first four layers of the (2×6) and (4×2) reconstructions are 0.7 and 1.2. Consequently, the As/Ga ratio is lower for the (2×6) than for the (4×2), in agreement with the XPS results.

As shown in Table I, a range of XPS $2p_{3/2}$ area ratios are observed for the $c(4\times4)$, $c(2\times8)$, and $c(8\times2)$ reconstructions. This may result from the existence of several atomic structures with the same unit cell size, for example, models (c) and (d) for the $(2\times4)/c(2\times8)$ in Fig. 1. Alternatively, the composition variation may result from the occurrence of mixed surface phases that are not discernable in the LEED pattern. As discussed below, the STM images of the (4×2) surface always show the presence of some (2×6) domains.

A. $c(4\times4)$ reconstruction

Shown in Fig. 2(a) is an STM picture of the $c(4\times4)$ reconstruction. The staggered gray patches are due to the top layer of arsenic dimers. Inspection of the images reveals that there are two different $c(4\times4)$ structures, one in which there are three As dimers in a row, and one in which there are two As dimers in a row. In the former case, the gray patches are elongated in the $[\bar{1}10]$ direction, whereas in the latter case, the gray patches are square. Some of these features are highlighted with black rectangles and squares in the image. The results presented here are consistent with those reported previously for the $c(4\times4)$ reconstruction.[5]

Upon exposing the $c(4\times4)$ to a flux of hydrogen atoms

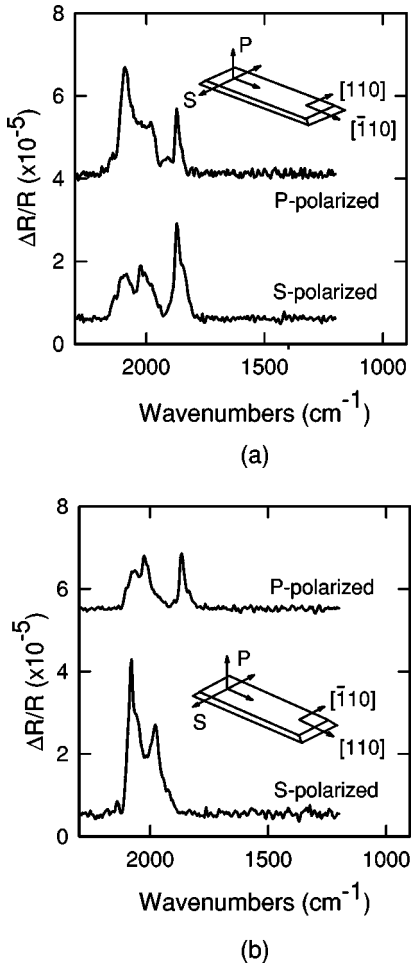

FIG. 3. Polarized infrared reflectance spectra of hydrogen adsorbed on the $c(4\times4)$ surface, with the long crystal axis parallel to the [110] direction in (a) and the [110] direction in (b).

at 300 K, the LEED pattern gradually shifts to (1×1), and the XPS As $2p_{3/2}$/Ga $2p_{3/2}$ area ratio declines from 2.0 to 1.6. These data indicate that hydrogen reacts with the arsenic exposed on the surface, and etches some fraction of it away. Previous studies of hydrogen atom adsorption on the $c(4\times4)$ have obtained similar results.[38,39] In addition, these studies have shown that at much higher dosages, ~10 000 L, the surface becomes Ga-rich and exhibits a rough morphology.

Shown in Fig. 3 are polarized infrared reflectance spectra of hydrogen adsorbed on the $c(4\times4)$ surface. The inset diagrams indicate the electric field vectors for the polarized light, and show the two orientations of the crystals used in the experiments. These spectra contain a series of overlapping bands in the frequency range between 2200 and 1900 cm^{-1}, which can be assigned to arsenic hydrides. This assignment is made by comparison to the vibrational spectra of known arsenic hydride molecules, such as AsH_3.[9] Examination of the spectra in Fig. 3 reveals that the As–H stretching vibrations are more intense when the light is polarized parallel to the [110] crystal axis. Note that in the *s*-polarized spectrum of Fig. 3(b) these bands exhibit sharp maxima at 2080 and 1980 cm^{-1}.

In addition to the As–H bands, a gallium hydride stretching vibration is observed at 1865 cm^{-1} (Ref. 9). This peak is completely absent from the *s*-polarized infrared spectrum, indicating that the dipole moment for the Ga–H stretch must lie within the plane swept out by the [001] and [110] crystal axes. The observation of a Ga–H infrared band provides further evidence that the top layer of As atoms is etched from the $c(4\times4)$ surface upon exposure to hydrogen atoms at 300 K.

B. (2×4) reconstruction

Shown in Fig. 2(b) is an STM image of the $(2\times4)/c(2\times8)$ reconstruction. The unit cell consists of two arsenic dimers (set of four white spots) next to two dimer vacancies (dark region). The As dimers form rows that extend along the [110] direction. The As $2p_{3/2}$/ Ga $2p_{3/2}$ area ratio measured for this surface is 1.4, indicating that it has the maximum possible As coverage for a (2×4) phase. Accordingly, this reconstruction most likely corresponds to model (c) in Fig. 1.

In addition to the pairs of As dimers, a number of other features are evident in the STM image. Some (2×4) unit cells contain 0, 1, or 3 As dimers, and occasionally, a single As atom replaces one of the dimers. Also, there are bright white patches sitting on top of the As dimer rows. These patches probably are due to adsorbed arsenic. Typically, less than 2% of the surface area of the (2×4) is covered with the white patches. It should be pointed out that in large-scale STM images, three As-terminated layers are observed.[10] All three layers are (2×4) reconstructed and are separated by double-height steps.

During dosing with hydrogen atoms, the (2×4) gradually changes to (1×4). Scanning tunneling micrographs taken at saturation coverage reveal rows with $\times4$ periodicity, but no structure can be discerned within the rows. Another STM study has been conducted of hydrogen adsorption on the (2×4), but the quality of the images makes it difficult to unambiguously identify the atomic structure within the rows.[40] These results and other published work[38,39] indicate that hydrogen adsorption lifts the $\times2$ symmetry imposed by the arsenic dimer bonds. On the other hand, x-ray photoemission spectra collected by us after hydrogen dosing show no significant change in the As/Ga ratio, so arsenic etching of the (2×4) can be ruled out under our experimental conditions.

Shown in Fig. 4 are polarized infrared reflectance spectra of hydrogen adsorbed at saturation coverage on the (2×4) surface. These spectra are similar to the ones published before for surfaces prepared by wet chemical etching and annealing, except that the present spectra exhibit better signal-to-noise ratios.[9] The overlapping bands observed between 2200 and 1900 cm^{-1} are assigned to arsenic hydride stretching vibrations, while the two sharp peaks observed at 1880 and 1835 cm^{-1}, and the broad shoulder seen at 1750 cm^{-1}, are due to gallium hydride stretching vibrations. The As–H vibrational bands are strongly *p*-polarized when the long axis of the crystal is parallel to the [110] direction, whereas they are strongly *s*-polarized when the long axis of the crystal is parallel to the [110] direction. The intensities of the Ga–H vibrational bands are strongly dependent on the

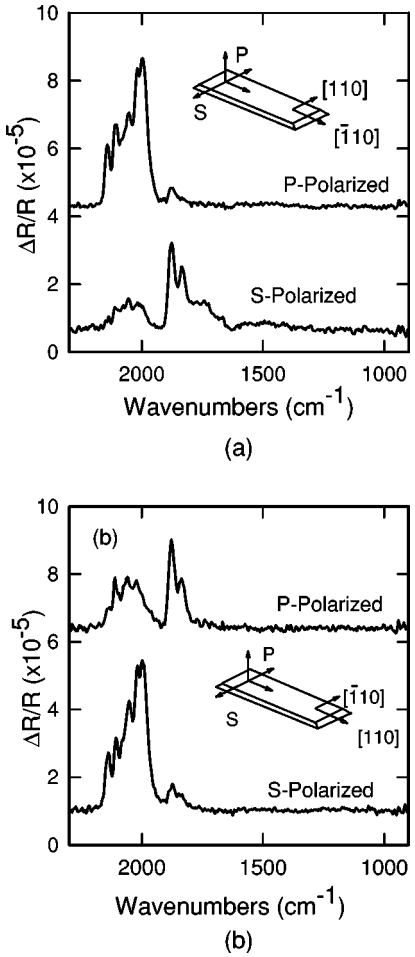

FIG. 4. Polarized infrared reflectance spectra of hydrogen adsorbed on the (2×4) surface, with the long crystal axis parallel to the [110] direction in (a) and the [110] direction in (b).

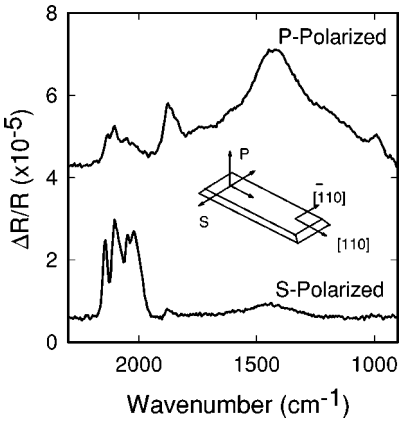

FIG. 5. Polarized infrared reflectance spectra of hydrogen adsorbed on the (2×6) surface, with the long crystal axis parallel to the [110] direction.

polarization as well, but in the opposite direction of the As–H spectra. We have interpreted these results to mean that the As–H and Ga–H dipole moments mainly lie within the (110) and ($\bar{1}$10) planes, respectively.[9] However, some rotation out of these planes is evident from inspection of the data: the intensities of the As–H vibrational bands are not zero in the *s*-polarized spectrum in Fig. 4(a), nor are the intensities of the Ga–H vibrational bands zero in the *s*-polarized spectrum in Fig. 4(b). The adsorption sites corresponding to the different infrared bands observed are discussed later.

C. (2×6) reconstruction

Presented in Fig. 2(c) is an STM image of the (2×6) GaAs(001) surface. One sees single rows of arsenic dimers (white oblong shapes) that are separated from each other in the [110] direction by 24 Å. The As dimers within the rows are not well ordered, and randomly shift one lattice spacing to the left or right of the row axis. This image is in good agreement with other STM studies of the (2×6).[3,5] Model (e) in Fig. 1, proposed by Biegelsen *et al.*,[3] is consistent with these and other experimental results. Note that their model assumes that zigzagging chains of Ga dimers are located in between the As dimer rows. While the STM image does show gray spots within the dark regions, it is not possible to definitively assign these features to gallium dimers.

Scanning tunneling micrographs obtained over larger areas reveal that up to three layers of the crystal are exposed on the (2×6) surface.[10] Most of these layers are (2×6) terminated, and are separated from each other by steps two atomic layers in height. Depending on the preparation conditions, the size of each terrace can vary from about 50 to 500 Å across. Also, it is not possible to prepare a pure (2×6) phase. Under the best circumstances, the (2×6) comprises about 80% of the GaAs (001) surface, while the remaining 20% is made up of (4×2) domains.

Shown in Fig. 5 are polarized infrared reflectance spectra of hydrogen adsorbed on the (2×6) reconstruction. The *s*-polarized spectrum contains a series of relatively intense bands between 2200 and 1950 cm^{-1} that are due to As–H stretching vibrations. These bands exhibit four main peaks at 2140, 2100, 2050, and 2020 cm^{-1}. Similar bands are seen in the *s*-polarized spectrum of the hydrogen-terminated (2×4) surface [Fig. 4 (b)]. However, in the latter case, the peaks at 2140 and 2100 cm^{-1} are much less intense relative to the peaks at 2050 and 2020 cm^{-1}.

Examination of the *p*-polarized spectrum in Fig. 5 reveals an asymmetric band between 1950 and 1800 cm^{-1} that is attributed to terminal Ga–H stretching vibrations. In addition, there is an extremely broad band centered at 1420 cm^{-1}, which overlaps with other broad peaks at approximately 1740, 1620, 1190, and 1000 cm^{-1}. These strongly *p*-polarized infrared bands are assigned to the asymmetric stretching vibrations of bridging gallium hydrides.[9] The polarization is consistent with the asymmetric stretch occurring parallel to the [110] crystal axis. The bridging gallium hydrides are formed by the insertion of H atoms into Ga dimer bonds. Consequently, the observation of these broad, low-frequency bands provides direct experimental confirmation of the presence of gallium dimers on the (2×6) surface. Note that the region between 1700 and 1000 cm^{-1} is completely flat in the reflectance spectra of adsorbed hydrogen on the $c(4\times4)$ and (2×4) reconstructions.

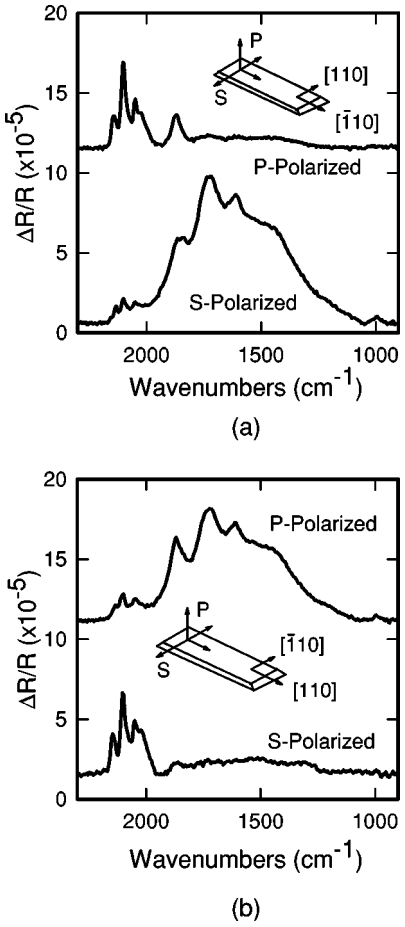

FIG. 6. Polarized infrared reflectance spectra of hydrogen adsorbed on the (4×2) surface, with the long crystal axis parallel to the [110] direction in (a) and the [110] direction in (b).

D. (4×2) reconstruction

In Fig. 2(d), an STM image is presented of the (4×2) reconstruction. This picture shows a series of double rows of light gray spots that extend along the [110] direction (some are highlighted with black dots in the image). The spot spacing is 4 Å along the rows, and the distance between the double rows is 16 Å, as expected for the (4×2) cell. Based on STM studies and total energy calculations, model (g) in Fig. 1 is the correct structure for this surface.[3,5,7] The gray spots seen in the filled-states image are associated with the second-layer arsenic atoms underneath the gallium dimers.[5]

It should be pointed out that it is not possible to anneal the gallium arsenide crystal such that only the (4×2) phase is present. Large-scale images reveal that for the annealing conditions used in our study, approximately 80% of the surface is (4×2) with the remainder (2×6).[10] Also, one sees a small concentration of white blobs (<1% of the area) that are believed to be gallium clusters. These clusters precipitate out on the surface when the (4×2) is created from the (2×6) during annealing.

Presented in Fig. 6 are polarized infrared reflectance spectra of hydrogen adsorbed on the (4×2) surface. The *p*-polarized spectrum in (a) and the *s*-polarized spectrum in (b) contain three sharp peaks at 2140, 2100, and 2050 cm^{-1}, and a shoulder at 2020 cm^{-1}, which are due to arsenic hydride vibrations. These bands are similar to those seen for hydrogen adsorption on the (2×6) reconstruction, except that in the case of the (4×2), the peaks at 2100 and 2050 cm^{-1} are of higher relative intensity compared to the other features.

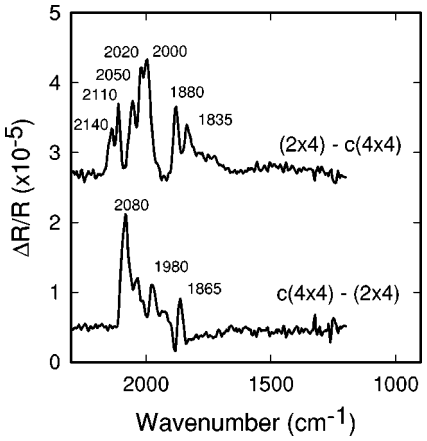

FIG. 7. Subtraction of the infrared reflectance spectra of the $c(4\times4)$ from the (2×4) and vice versa.

Between about 1950 and 950 cm^{-1} a series of broad overlapping bands are seen in the *s*-polarized spectrum of Fig. 6(a) and the *p*-polarized spectrum of Fig. 6(b). The maximum observed at about 1875 cm^{-1} is assigned to terminal gallium hydride vibrations, while the remaining features with maxima at 1730 and 1605 cm^{-1}, and a prominent shoulder at 1480 cm^{-1}, are due to the asymmetric stretching modes or bridging gallium hydride.[9] These latter modes result from hydrogen adsorption onto the Ga dimers which terminate the (4×2) surface. The absence of band intensity in the *p*-polarized reflectance spectrum of Fig. 6(a) indicates that the asymmetric mode for the bridging hydride is directed parallel to the [110] crystal axis. Note that there are significant differences in the location, size, and shape of the bridging hydride infrared bands for the (4×2) and (2×6) surfaces. The origin of these differences is discussed in the next section.

IV. DISCUSSION

A. Arsenic-rich surfaces, $c(4\times4)$ and (2×4)

Our experimental results indicate that on the $c(4\times4)$ surface, hydrogen atoms etch away the top layer of arsenic and bond to the second layer of arsenic atoms that are exposed underneath. Consequently, one expects that the sites for hydrogen adsorption on the $c(4\times4)$ reconstruction should be similar to those on the (2×4) reconstruction. To test this hypothesis, we subtracted the infrared reflectance spectrum of the hydrogen-terminated $c(4\times4)$ from the infrared reflectance spectrum of the hydrogen-terminated (2×4), and vice versa. These results are presented in Fig. 7. They show that contrary to expectation, the infrared peaks are located at different frequencies for the two structures. On the $c(4\times4)$, the dominant vibrational bands occur at 2080, 1980, and 1865 cm^{-1}, whereas on the (2×4), a greater number of bands are recorded at 2140, 2110, 2050, 2020, 2000,

1880, and 1835 cm^{-1}. Evidently, the frequencies of the As–H and Ga–H stretching vibrations are sensitive to the arrangement of the arsenic atoms on the top layer of the crystal.

Chabal and co-workers[41] have shown that hydrogen can adsorb onto Si (100) in a variety of different bonding configurations, including isolated monohydrides, coupled monohydrides (Si_2H_2), dihydrides, and on rough surfaces, even trihydrides. The first three of these could also occur on the surface of GaAs (001). The coupled monohydrides and dihydrides exhibit asymmetric and symmetric stretching vibrations that are parallel and perpendicular to the crystal surface. For Si (100), the latter mode produces a more intense infrared band that is always *p*-polarized regardless of the crystal orientation. Chabal *et al.*[41] have pointed out that the symmetric mode undergoes dielectric screening by the crystal surface, which reduces its reflectance intensity relative to that of the asymmetric mode. The screening is proportional to the square of the electric polarizability, which for H:Si (100) is about 2.0. Since the screening is not that large, it is relatively straightforward to identify the asymmetric and symmetric vibrations of the couple monohydrides and dihydrides on the silicon surface.

We anticipate that the polarizability of hydrogen-terminated gallium arsenide may be significantly greater than that for H:Si (100), because the Ga and As atoms are larger than the Si atoms.[42] Also, the dielectric constant of gallium arsenide is greater than that of silicon.[43] Consequently, the symmetric stretching vibrations may be much weaker than the asymmetric stretching vibrations, making them difficult to extract from the infrared spectrum. Careful inspection of the data shown in Figs. 3 and 4 does not reveal any bands that are exclusively *p*-polarized independent of the crystal orientation. Instead, the As–H stretching vibrations tend to be strongly *p*-polarized when the long crystal axis is parallel to the [110] direction and strongly *s*-polarized when the long crystal axis is parallel to the [110] direction. This suggests that the infrared peaks are more likely due to isolated arsenic monohydrides. However, because it is not currently possible to calculate the extent of the dielectric screening, we cannot rule out the existence of coupled arsenic monohydrides and arsenic dihydrides. It should be noted that isotope mixing experiments were carried out as well, but decoupling was not observed in any of the bands as the adsorbed hydrogen was diluted in adsorbed deuterium. This provides further support for assigning all the As–H infrared bands to monohydrides.

The observation of seven peaks at different frequencies means that there are seven distinct chemical environments for the arsenic monohydrides on the As-rich reconstructions. Each environment is determined by a unique coordination of atoms about the arsenic adsorption site. To illustrate these different possibilities, we present ball-and-stick models for the hydrogen-terminated $c(4\times4)$ and (2×4) surfaces in Fig. 8. These sites are labeled 1–8. The most common hydride configuration is one in which the arsenic atom is bonded to a hydrogen atom and two gallium atoms, and contains a lone pair of electrons in its remaining dangling bond (site 1). This arsenic monohydride is generated by displacement of an As dimer from the $c(4\times4)$, or by addition of hydrogen across

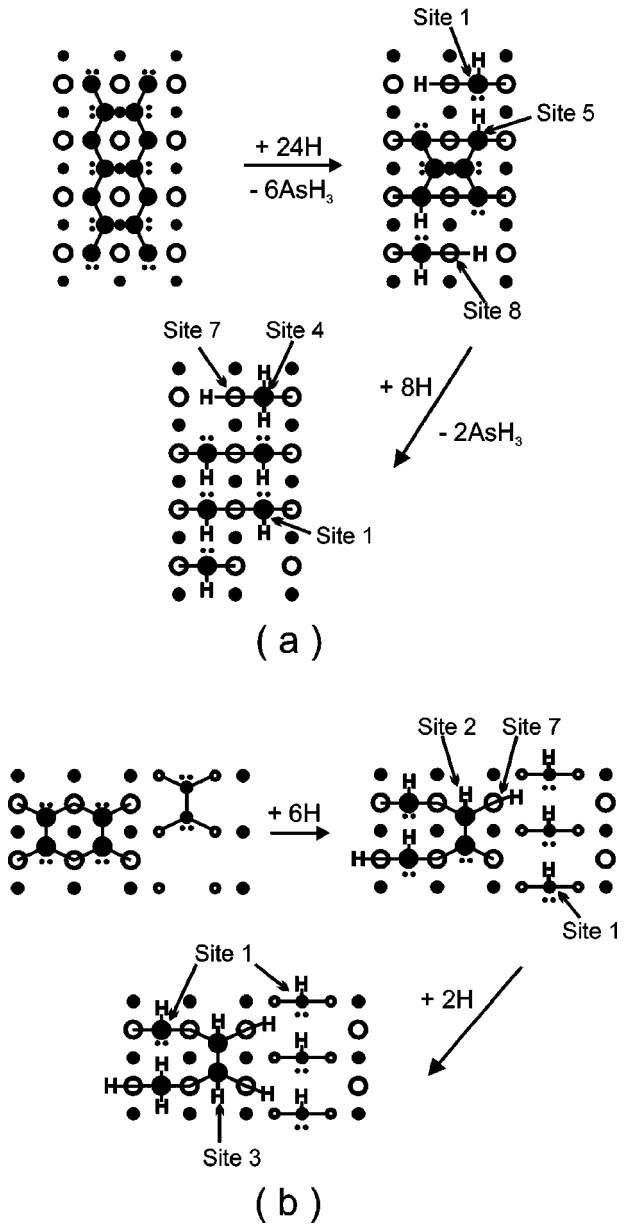

FIG. 8. Ball-and-stick models for hydrogen adsorption on the $c(4\times4)$ and (2×4) surfaces.

an As dimer bond on the (2×4). Notice that the H atom may be located within about 3 Å of an adjacent As atom with a lone pair of electrons. This is sufficiently close for weak hydrogen bonding to occur. Thus, for this species, two vibrational frequencies may be observed, corresponding to isolated and hydrogen-bonded arsenic monohydride.

Site 2 in Fig. 8 illustrates another monohydride configuration. In this case, the central As atom is bonded to an H atom, an As atom, and two Ga atoms (i.e., the As dimer bond remains intact). This monohydride is produced by the attack of two H atoms across the As–Ga bond, making As–H and Ga–H species. Site 2 is more likely to occur on the (2×4) surface, where the second-layer Ga atoms are exposed along the edges of the arsenic dimer rows. Addition of H atoms to an As–Ga bond on the opposite end of the As dimer will produce a coupled monohydride (site 3). Hydrogen atoms could also attack the As–Ga bond of an isolated monohy-

dride with a lone pair of electrons (site 1), and convert it into a dihydride (site 4).

Two other coordination environments that may occur on the $c(4\times4)$ and (2×4) surfaces are hydrides bonded to arsenic atoms located in the second or lower layers. In this case, the As atom may be bonded to one As atom above and two Ga atoms below, as indicated by site 5 in Fig. 8. Alternatively, the As atom may be bonded to three Ga atoms, one above and two below (site 6). This site might be found below the edge of double-height steps. Also shown in Fig. 8 are two gallium hydrides, labeled sites 7 and 8. These are formed by adsorption of hydrogen on second-layer Ga atoms. The two sites differ in the type of top-layer arsenic atom that coordinates with the gallium atom.

Since detailed simulations of the hydrogen-terminated surface would be required to make definitive assignments, we can only speculate as to the exact adsorption site corresponding to each infrared band. However, an indication of the ranges of vibrational frequencies for each type of hydride can be obtained by comparison to the infrared spectra of gaseous arsenic compounds.[44–46] Arsine, ethylarsine, tertiarybutylarsine, and diethylarsine exhibit As–H stretching vibrations in the following ranges: AsH_3, 2123 and 2116 cm^{-1}; $EtAsH_2$, 2107–2086 cm^{-1}; $tBuAsH_2$, 2126–2088 cm^{-1}; and Et_2AsH, 2080 cm^{-1}. In addition, in the arsine–trimethylgallium adduct, the As–H vibrations are shifted 40 cm^{-1} higher in frequency compared to arsine.[47] This shift is due to the conversion of the nonbonding pair of electrons into a dative bond between As and Ga. The lone pair of electrons on the As atom tends to weaken the As–H bond. Based on the foregoing discussion, we tentatively assign the different arsenic hydrides to specific frequency ranges as follows: 2150 to 2105 cm^{-1}, dihydrides, coupled monohydrides, and isolated monohydrides on intact As dimers (sites 2, 3, and 4); 2105 to 2040 cm^{-1}, monohydrides bound to second-layer As atoms (sites 5 and 6); and 2040 to 1950 cm^{-1}, isolated monohydrides bound to top-layer As atoms with lone paris of electrons (site 1).

In spite of the complexity of the reflectance spectra for adsorbed hydrogen on the $c(4\times4)$ and (2×4) surfaces, all the features observed can be ascribed to three main adsorption sites: As dimers, second-layer Ga atoms, and second-layer As atoms. Moreover, the infrared spectra and the (1×1) and (1×4) LEED patterns can be readily explained by the adsorption models presented in Fig. 8, and are consistent with structure (a) for the $c(4\times4)$ and structure (c) for the (2×4) as given in Fig. 1.

B. Gallium-rich surfaces, (2×6) and (4×2)

The infrared spectra of adsorbed hydrogen on the (2×6) and (4×2) reconstructions contain an additional feature that is not seen on the As-rich surfaces. This is the extremely broad band extending from about 1800 to 950 cm^{-1}, which is due to bridging gallium hydride. The bridged hydride inserts between the Ga dimer atoms and makes a 3-center–2-electron bond. Since the H atom brings one electron with it, a second hydrogen must coordinate to the terminal position on the Ga dimer. Otherwise, an odd number of electrons would occupy the hydride bond orbitals.

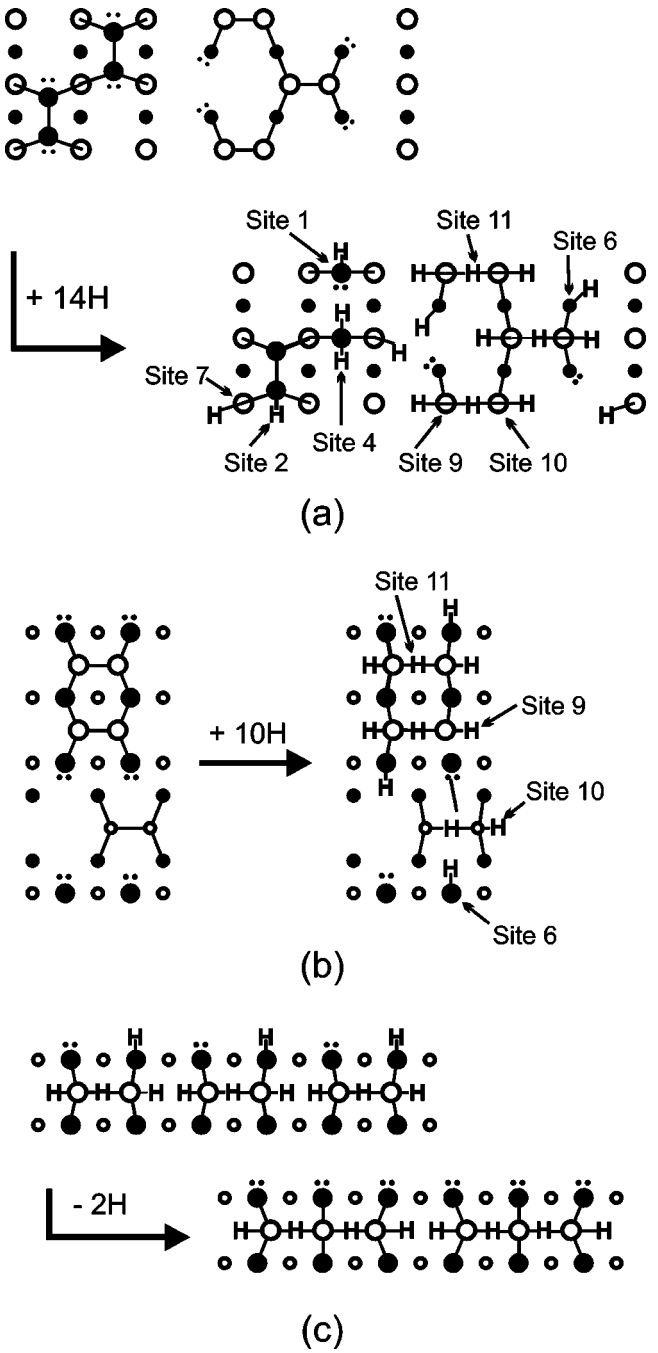

FIG. 9. Ball-and-stick models for hydrogen adsorption on the (2×6) and (4×2) surfaces.

Shown in Figs. 9(a) and 9(b) are proposed ball-and-stick models for the hydrogen-terminated (2×6) and (4×2) surfaces. The gallium dimers provide three additional sites for hydrogen adsorption: site 11, bridged; and sites 9 and 10, terminal. The two terminal sites differ slightly in the coordination sphere of the gallium atom. The gallium at site 9 is bonded to an As atom with a lone pair of electrons in its dangling-bond orbital, while the gallium at site 10 is bonded to an As atom that is beneath the surface and fully coordinated to other Ga atoms. The models of the Ga-rich surfaces contain another arsenic monohydride that does not show up in the models of the As-rich surfaces. It is denoted as site 6 in the figure and results from hydrogen adsorption onto

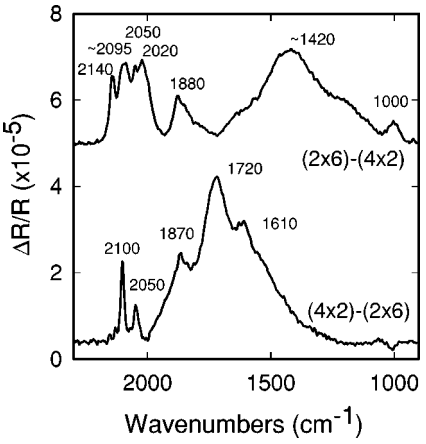

FIG. 10. Subtraction of the infrared reflectance spectra of the (4×2) from the (2×6) and vice versa.

second-layer As atoms that are exposed along the edges of the Ga dimer rows. In this case, the central As atom is coordinated to hydrogen and three Ga atoms. This site must become occupied simultaneously with the terminal position of the adjoining Ga dimer, so as to avoid filling the hydride bond orbitals with an odd number of electrons.

The (2×6) is a unique reconstruction because it is terminated with both arsenic and gallium dimers. Consequently, it contains all the hydride coordination sites, except site 5, which is associate with the $c(4\times4)$ phase. Perusal of Fig. 5 reveals that the infrared spectra of the H-terminated (2×6) contain a series of As–H and Ga–H vibrational bands that are characteristic of hydrogen adsorption onto As and Ga dimers. The infrared spectra of the H-terminated (4×2) shown in Fig. 6 also contain As–H and Ga–H bands characteristic of adsorption on As and Ga dimers. However, this may be explained by the coexistence of (2×6) domains on the (4×2) surface. As stated earlier, STM images indicate that the most Ga-rich surfaces are composed of no more than 80% (4×2), with the remainder (2×6).

In order to delineate the hydrogen adsorption sites corresponding to each Ga-rich reconstruction, we have subtracted the reflectance spectrum of the H:(2×6) from that of the H:(4×2) and vice versa. These results are presented in Fig. 10. Subtraction of the (2×6) from the (4×2) eliminates all but two bands from the As–H stretching region, located at 2100 and 2050 cm^{-1}. We propose that these relatively narrow peaks are due to hydrogen adsorption on second-layer arsenic atoms (site 6). At this time, we cannot explain why there are two peaks. Possibly they are associated with step and terrace sites. Finally, it should be pointed out that models (f) and (g) in Fig. 1 are compatible with our infrared results, whereas model (h) is not.

Further examination of the infrared spectra in Fig. 10 reveals that the asymmetric stretching vibrations of the bridging gallium hydrides are at significantly different frequencies on the two surfaces. For the (2×6), the broad low-frequency band exhibits a maximum at about 1420 cm^{-1} with well-defined shoulders at 1620 and 1190 cm^{-1}. In addition, a small band is present at 1000 cm^{-1}. By contrast, the bridging band for the (4×2) contains two overlapping peaks centered at 1720 and 1610 cm^{-1}. (The third peak at 1870 cm^{-1} is due to the stretching vibrations of terminal gallium hydrides.) The frequency of the bridging band is related to the Ga–H–Ga bond angle, and in turn, the average Ga–Ga bond distance. Assuming that the Ga atoms are rigidly held in place, then the vibrational frequency of the asymmetric stretch is approximately given by the following relationship:[48]

$$\nu_{\mathrm{as}}=(k_r/2\pi^2 m_H)^{1/2}\sin(\theta/2), \tag{1}$$

where k_r is the force constant, m_H is the mass of atomic hydrogen, and θ is the Ga–H–Ga bond angle. Since the ν_{as} values are higher on the (4×2) than on the (2×6), one can conclude that the bond angles are larger on the former reconstruction.

The difference in the Ga–H–Ga bond angles may be related to the structures of the Ga dimer rows on the two reconstructions. On the (2×6), the gallium dimers are interspersed between disordered rows of arsenic dimers, whereas on the (4×2), the gallium dimers extend in long rows along the [110] direction. One possibility is that the dimers on the (4×2) surface couple with one another to form trimers, as shown in Fig. 9(c). This coupling is not possible on the (2×6). Digallane (Ga_2H_6) exhibits similar behavior when it is condensed into a thin solid film at 77 K.[49] The molecule undergoes oligomerization, resulting in an increase in the Ga–H–Ga bond angle from 98 to 122 deg. The oligomerized gallane exhibits a broad infrared band for the asymmetric stretching mode of the bridging hydride that is analogous to that seen for the bridging hydride on the (4×2): the band is centered at 1705 cm^{-1} and has a full-width-at-half-maximum of ~150 cm^{-1}. Amorphous hydrogenated gallium arsenide also exhibits a broad infrared band for bridging Ga–H–Ga.[50] In this case, the band is centered at 1420 cm^{-1}, and is similar in relative size and shape to the low-frequency hydride band observed for the (2×6) surface (top spectrum in Fig. 10).

The asymmetric stretching modes for bridging gallium hydride on GaAs (001) range in frequency from 1720 to 1000 cm^{-1}. This indicates that there is a large variation in the Ga–H–Ga bond angles on the crystal surface. For example, for gaseous digallane, the bond angle is 98 deg and the asymmetric stretch is at 1273 cm^{-1}, whereas for condensed digallane, the bond angle is 122 deg and the asymmetric stretch is at 1705 cm^{-1} (Ref. 51). The frequencies observed for the bridging species on the GaAs (001) surface could easily encompass a range of angles from 125 to 90 deg. If one assumes a constant Ga–H bond length of 1.7 Å,[50,51] then these angles correspond to Ga–Ga distances ranging from 3.0 to 2.4 Å.

The bridging hydride should also exhibit a symmetric stretching vibration that is perpendicular to the crystal surface. In digallane, this mode occurs between 1200 and 900 cm^{-1} (Ref. 51). Inspection of Figs. 5 and 6 does not reveal any peaks that are exclusively *p*-polarized in this frequency range. There are several reasons why we might not be able to detect this mode. The intensity of the symmetric mode is generally much weaker than that of the asymmetric mode for Ga–H–Ga bond angles in excess of 100 deg.[48,52] In addition,

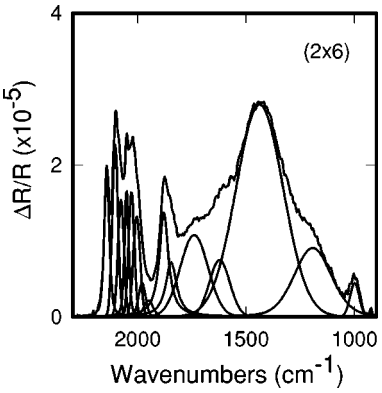

FIG. 11. Deconvolution of the overlapping bands in the infrared reflectance spectra of adsorbed hydrogen on the (2×6) and (4×2) surfaces.

dielectric screening by the GaAs surface may greatly reduce the intensity of the symmetric mode.

C. Deconvolution of the reflectance spectra

The infrared reflectance spectra for the hydrogen-terminated (2×6) and (4×2) surfaces have been deconvoluted to determine the position and full-width-at-half-maximum (FWHM) for each peak. These results are presented in Fig. 11 and Table II. One sees that the FWHMs for the As–H stretching vibrations vary from 23 to 38 cm^{-1}. For arsine isolated within an argon matrix at 12 K, the FWHM of the As–H stretching vibration is 25 cm^{-1} (Ref. 53). This value is comparable to that for the surface arsenic hydrides, and indicates that the line widths for these latter species are intrinsic to the As–H harmonic oscillator. The larger FWHMs measured by us are probably due to the much higher sample temperature (300 K), which decreases the lifetime of the excited state, and broadens the line.

TABLE II. Characteristics of the infrared peaks for adsorbed hydrogen on GaAs (2×6) and (2×4) surfaces.

		(2×6)		(4×2)	
Stretching mode	Frequency (cm^{-1})	Area ($\times 10^2$ cm−1)	FWHM (cm^{-1})	Area ($\times 10^2$ cm^{-1})	FWHM (cm^{-1})
As–H	2142	2.09	28	1.07	28
As–H	2103	2.30	31	3.44	31
As–H	2078	1.62	32	1.17	32
As–H	2051	1.48	23	1.19	23
As–H	2028	1.68	31	1.29	31
As–H	2002	1.53	36	0.72	36
As–H	1980	0.57	38	0.26	38
$Ga–H_T$	1950	0.37	50	1.25	50
$Ga–H_T$	1878	3.26	51	5.53	51
$Ga–H_T$	1843	2.02	61	1.54	61
$Ga–H_B$	1729	⋯	⋯	16.5	151
$Ga–H_B$	1740	5.38	151	⋯	⋯
$Ga–H_B$	1604	⋯	⋯	7.10	110
$Ga–H_B$	1622	2.74	111	⋯	⋯
$Ga–H_B$	1481	⋯	⋯	19.6	256
$Ga–H_B$	1437	23.6	256	⋯	⋯
$Ga–H_B$	1253	⋯	⋯	3.44	200
$Ga–H_B$	1192	6.38	202	⋯	⋯
$Ga–H_B$	995	0.73	50	0.21	50

The full-width-at-half-maxima for the terminal and bridged gallium hydrides (GaH_T and GaH_B) are significantly larger than those for the arsenic hydrides. The FWHM for the bridging mode ranges from 50 to 256 cm^{-1}. As already stated, these line widths are similar to those recorded for this same mode in condensed digallane and amorphous hydrogenated gallium arsenide.[49–51] The broad line shape is probably due to the existence of a continuous distribution of Ga–H–Ga bond angles about the mean, and to a lesser extent, to anharmonic interactions among the different vibrational modes.[41]

V. SUMMARY AND IMPLICATIONS

Our study has shown that many different arsenic and gallium hydrides are produced upon hydrogen adsorption onto the GaAs (001) surface. For example, seven vibrational bands, at frequencies ranging from 2150 to 1950 cm^{-1}, are observed following hydrogen termination of arsenic dimers and second-layer arsenic atoms. These seven bands are indicative of seven distinct adsorption sites, in which the coordination sphere of the As atoms changes. With regard to gallium sites, there are eight vibrational bands, corresponding to an equal number of different chemical environments.

These results have important implications for the surface chemistry of gallium arsenide. Several studies have shown that chemical reactions occurring during the processing of this material are ''site-specific.'' [9,35,54] This specificity may manifest itself upon adsorption. For example, on the (2×4) reconstruction, arsine only adsorbs onto the second-layer Ga atoms.[35] Alternatively, it may manifest itself through a surface reaction, such as when the chlorine ligands of CCl_4 react with exposed Ga atoms and desorb GaCl.[54] As the present study demonstrates, infrared spectroscopy of adsorbed hydrogen is unsurpassed in its ability to distinguish among the many different sites present on the gallium arsenide surface. By using hydrogen titration of adsorption sites in conjunction with scanning tunneling microscopy and other surface-science techniques, we should be able to greatly improve our understanding of the site-specific chemistry of processing compound semiconductors into solid-state devices.

ACKNOWLEDGMENTS

Funding for this research was provided by the Office of Naval Research (Grant No. N00014-95-1-0904), and by the National Science Foundation, Chemical and Thermal Systems (Grant No. CTS-9531785) and Division of Materials Research (Grant No. DMR-9804719).

[1] P. K. Larsen, J. H. Neave, J. F. van der Veen, P. J. Dobson, and B. A. Joyce, Phys. Rev. B **27**, 4966 (1983).
[2] G. Qian, R. M. Martin, and D. J. Chadi, Phys. Rev. Lett. **60**, 1962 (1988); P. K. Larsen and D. J. Chadi, Phys. Rev. B **37**, 8282 (1988); G. Qian, R. M. Martin, and D. J. Chadi, *ibid.* **38**, 7649 (1988); D. J. Chadi, J. Vac. Sci. Technol. A **5**, 834 (1987).
[3] D. K. Biegelsen, R. D. Bringans, J. E. Northrup, and L. E. Swartz, Phys. Rev. B **41**, 5701 (1990).
[4] M. D. Pashley, K. W. Haberern, and J. M. Gaines, Surf. Sci. **267**, 153 (1992); M. D. Pashley, K. W. Haberern, and J. M. Woodall, J. Vac. Sci. Technol. B **6**, 1468 (1988); M. D. Pashley, K. W. Haberern, and W. Friday, Phys. Rev. Lett. **60**, 2176 (1988).
[5] T. Hashizume, Q. K. Xue, A. Ichimiya, and T. Sakurai, Phys. Rev. B **51**,

4200 (1995); Q. K. Xue, T. Hashizume, J. M. Zhou, T. Sakata, T. Sakurai, and T. Ohno, Phys. Rev. Lett. **74**, 3177 (1995).
[6] M. Wassermeier, V. Bressler-Hill, R. Maboudian, K. Pond, X. S. Wang, W. H. Weinberg, and P. M. Petroff, Surf. Sci. Lett. **278**, L147 (1992); V. Bressler-Hill, M. Wassermeier, K. Pond, R. Maboudian, G. A. D. Briggs, P. M. Petroff, and W. H. Weinberg, J. Vac. Sci. Technol. B **10**, 1881 (1992).
[7] J. E. Northrup and S. Froyen, Mater. Sci. Eng., B **30**, 81 (1995); Phys. Rev. B **50**, 2015 (1994); Phys. Rev. Lett. **71**, 2276 (1993).
[8] J. Falta, R. M. Tromp, M. Copel, G. D. Pettit, and P. K. Kirchner, Phys. Rev. Lett. **69**, 3068 (1992).
[9] H. Qi, P. E. Gee, T. Nguyen, and R. F. Hicks, Surf. Sci. **323**, 6 (1995); H. Qi, P. E. Gee, and R. F. Hicks, Phys. Rev. Lett. **72**, 250 (1994); P. E. Gee and R. F. Hicks, J. Vac. Sci. Technol. A **10**, 892 (1992).
[10] L. Li, B. K. Han, S. Gan, H. Qi, and R. F. Hicks, Surf. Sci. **398**, 386 (1998).
[11] J. Falta, R. M. Tromp, M. Copel, G. D. Pettit, and P. D. Kirchner, Phys. Rev. B **48**, 5282 (1993); Phys. Rev. Lett. **69**, 3068 (1992).
[12] P. Drathen, W. Ranke, and K. Jacobi, Surf. Sci. **77**, L162 (1978).
[13] M. D. Pashley, Phys. Rev. B **40**, 10481 (1989).
[14] H. H. Farrell and C. J. Palmstron, J. Vac. Sci. Technol. B **8**, 903 (1990).
[15] D. J. Frankel, C. Yu, J. P. Harbison, and H. H. Farrell, J. Vac. Sci. Technol. B **5**, 1113 (1987).
[16] S. L. Skala, J. S. Hubacek, J. R. Tucker, J. W. Lyding, S. T. Chou, and K. Y. Cheng, Phys. Rev. B **48**, 9138 (1993).
[17] F. J. Lamelas, P. H. Fuoss, D. W. Kisker, G. B. Stephenson, P. Imperatori, and S. Brennan, Phys. Rev. B **49**, 1957 (1994).
[18] R. Z. Bachrach, R. S. Bauer, P. Chiaradia, and G. V. Hansson, J. Vac. Sci. Technol. **18**, 797 (1981).
[19] F. Stietz, S. Sloboshanin, H. Engelhard, T. Allinger, A. Goldmann, and J. A. Schaefer, Solid State Commun. **94**, 643 (1995); J. A. Schaefer, V. Persch, S. Stock, T. Allinger, and A. Goldmann, Europhys. Lett. **12**, 563 (1990).
[20] P. Alnot, J. Olivier, and C. S. Fadley, J. Electron Spectrosc. Relat. Phenom. **49**, 159 (1989).
[21] B. A. Joyce, J. H. Neave, P. J. Dobson, and P. K. Larsen, Phys. Rev. B **29**, 814 (1984).
[22] J. M. McCoy, U. Korte, P. A. Maksysm, and G. Meyer-Ehmsen, Phys. Rev. B **48**, 472 (1993).
[23] A. Y. Cho, J. Appl. Phys. **42**, 2074 (1971).
[24] H. Yamaguchi and Y. Horikoshi, Phys. Rev. B **44**, 5897 (1991).
[25] C. Deparis and J. Massies, J. Cryst. Growth **108**, 157 (1991).
[26] P. Friedel, P. K. Larsen, S. Gourrier, J. P. Cabanie, and W. M. Gerits, J. Vac. Sci. Technol. B **2**, 675 (1984).
[27] R. Duszak, C. J. Palmstrom, L. T. Florez, Y. Yang, and J. H. Weaver, J. Vac. Sci. Technol. B **10**, 1891 (1992).
[28] A. J. Van Bommel, J. E. Crombeen, and T. G. J. Van Oirschot, Surf. Sci. **72**, 95 (1978).
[29] M. A. Mendez, F. J. Palomares, M. T. Cuberes, M. L. Gonzalez, and F. Soria, Surf. Sci. **251/252**, 145 (1991).
[30] L. H. Duboise and G. P. Schwartz, Phys. Rev. B **26**, 794 (1982).
[31] V. Polyakov, A. Elbe, and J. A. Schaefer, Appl. Phys. A: Mater. Sci. Process. **60**, 567 (1995); T. Allinger, J. A. Schaefer, Ch. Stuhlmann, U. Beckers, and H. Ibach, Physica B **170**, 481 (1991); J. A. Schaefer, Appl. Phys. A: Solids Surf. **51**, 305 (1990).
[32] M. C. Gallagher, R. H. Prince, and R. F. Willis, Surf. Sci. **275**, 31 (1994).
[33] M. Kuball, D. T. Wang, N. Esser, M. Cardona, J. Zegenhagen, and B. O. Fimland, Phys. Rev. B **52**, 16337 (1995).
[34] M. Kasu and N. Kobayashi, J. Appl. Phys. **78**, 3026 (1995).
[35] H. Qi, P. E. Gee, and R. F. Hicks, Surf. Sci. **347**, 289 (1996); P. E. Gee, H. Qi, and R. F. Hicks, *ibid.* **330**, 135 (1995).
[36] B. K. Han, L. Li, Q. Fu, and R. F. Hicks, Appl. Phys. Lett. **72**, 3347 (1998).
[37] G. Somorjai, *Chemistry in Two Dimensions: Surfaces* (Cornell University Press, Ithaca, NY, 1981).
[38] F. Stietz, J. Woll, V. Persch, T. Allinger, W. Erfurth, A. Goldmann, and J. A. Schaefer, Phys. Status Solidi A **159**, 185 (1997); J. A. Schaefer, F. Stietz, J. Woll, H. S. Wu, H. Yu, and G. J. Lapeyre, J. Vac. Sci. Technol. B **11**, 1497 (1993); J. A. Schaefer, T. Allinger, C. Stuhlmann, U. Beckers, and H. Ibach, Surf. Sci. **251/252**, 1000 (1991).
[39] D. Pahlke, M. Arens, N. Esser, D. T. Wang, and W. Richter, Surf. Sci. **352–354**, 66 (1996); N. Esser, P. V. Santos, M. Kuball, M. Cardona, M. Arens, D. Pahlke, W. Richter, F. Stietz, J. A. Schaefer, and B. O. Fimland, J. Vac. Sci. Technol. B **13**, 1666 (1995); M. Arens, M. Kuball, N. Esser, W. Richter, M. Cardona, and B. O. Fimland, Phys. Rev. B **51**, 10923 (1995).
[40] M. Kuball, D. T. Wang, M. Cardona, J. Zegenhagen, and B. O. Fimland, Phys. Rev. B **52**, 16337 (1995).
[41] Y. J. Chabal, G. S. Higashi, K. Raghavachari, and V. A. Burrows, J. Vac. Sci. Technol. A **7**, 2104 (1989); Y. J. Chabal and K. Raghavachari, Phys. Rev. Lett. **53**, 282 (1984); *ibid.* **54**, 1055 (1985); Y. Chabal, Surf. Sci. Rep. **8**, 211 (1988); O. Jacob, Y. J. Chabal, and K. Raghavachari, Chem. Phys. Lett. **187**, 325 (1991); Y. J. Chabal, J. Vac. Sci. Technol. A **3**, 1448 (1985); Y. J. Chabal, A. L. Harris, K. Raghavachari, and J. C. Tully, Int. J. Mod. Phys. B **7**, 1031 (1993).
[42] L. Pauling, *The Nature of the Chemical Bond and the Structure of Molecules and Crystals; and Introduction to Modern Structure Chemistry* (Cornell University Press, Ithaca, NY, 1960), p. 605.
[43] C. Kittel, *Introduction to Solid State Physics* (Wiley, New York, 1996).
[44] J. Nishizawa and T. Kurabayashi, J. Electrochem. Soc. **130**, 413 (1983).
[45] S. P. Den Baars, B. Y. Maa, P. D. Dapkus, and A. Melas, J. Electrochem. Soc. **136**, 2067 (1989).
[46] D. Speckman, J. Cryst. Growth **116**, 48 (1992).
[47] E. A. Piocos and B. S. Ault, J. Am. Chem. Soc. **111**, 8978 (1989).
[48] G. Herzberg, *Molecular Spectra and Molecular Structure, Infrared and Raman Spectra of Polyatomic Molecules* (Van Nostrand Reinhold, New York, 1945), Vol. 2, p. 168.
[49] C. R. Pulham, A. J. Downs, M. J. Goode, D. W. H. Rankin, and H. E. Robertson, J. Am. Chem. Soc. **113**, 5149 (1991).
[50] Z. P. Wang, L. Ley, and M. Cardona, Phys. Rev. B **26**, 3249 (1982).
[51] P. L. Baxter, A. J. Downs, D. W. H. Rankinm, and H. E. Robertson, J. Chem. Soc. Dalton Trans. **1985**, 807; A. J. Downs, M. J. Goode, and C. R. Pulham, J. Am. Chem. Soc. **111**, 1936 (1989); P. L. Baxter, A. J. Downs, M. J. Goode, D. W. H. Rankinm, and H. E. Robertson, J. Chem. Soc. Dalton Trans. **1990**, 2873.
[52] M. W. Howard, U. A. Jayasooriya, S. F. A. Kettle, D. B. Powell, and N. Sheppard, J. Chem. Soc. Chem. Commun. **1979**, 18.
[53] R. T. Arlinghaus and L. Andrews, J. Chem. Phys. **81**, 4341 (1984).
[54] L. Li, S. Gan, B.-K. Han, H. Qi, and R. F. Hicks, Appl. Phys. Lett. **72**, 951 (1998); L. Li, H. Qi, S. Gan, B.-K. Han, and R. F. Hicks, Appl. Phys. A: Mater. Sci. Process. **66**, S501 (1998).